

Numerical methods and machine learning algorithms for solution of Inverse problems

Larisa Beilina*

Department of Mathematical Sciences, Chalmers University of Technology and
Gothenburg University, SE-42196 Gothenburg, Sweden

Approximate global convergence and Adaptive finite element method for solution of hyperbolic CIP

- Approximate global convergence
- Layer stripping algorithm with respect to pseudo-frequency for explicit reconstruction of the coefficient in hyperbolic CIP
- Two-stage numerical procedure
 - Stage 1.** Approximately globally convergent numerical method provides a good approximation for the exact solution.
 - Stage 2.** Adaptive Finite Element Method refines it.

- A new approach have been developed: approximately globally convergent numerical methods for Coefficient Inverse Problems for a hyperbolic and parabolic PDE with the first publication

L. Beilina, M. V. Klibanov, A globally convergent numerical method for some coefficient inverse problems with resulting second order elliptic equations, *SIAM Sci.Comp.*, V.31, N.1, 478-509, 2008.

L.Beilina, M.V.Klibanov, *Approximate Global Convergence and Adaptivity for Coefficient Inverse Problems*, Springer, ISBN 978-1-4419-7804-2, 2012.

- This approach works with single measurement data.
 - *Single measurement* means that either only a single position of the point source or only a single direction of the incident plane wave is considered.
- In our applications we are working with experimental data in military applications. CIPs with single measurement data are the most suitable ones for military applications: various dangers on the battlefield do not allow to arrange multiple measurements.

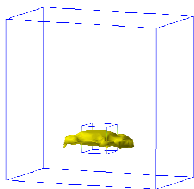
Main goals of the approximate globally convergent method

- **Goal 1.** To develop such a numerical method, which would have a rigorous guarantee obtaining a good approximation for the exact solution of an MCIP without using an advanced knowledge of neither a small neighborhood of that solution nor of the background medium in the domain of interest.
- **Goal 2.** This method should demonstrate a good performance on both computationally simulated and experimental data.
- It is *challenging* to achieve both goals simultaneously.
- Therefore some **approximate** mathematical models are necessary.

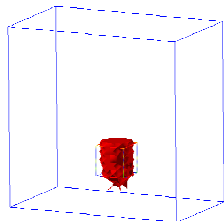
The two-stage numerical procedure

Stage 1. Approximately globally convergent numerical method provides a good approximation for the exact solution.

Stage 2. Adaptive Finite Element Method refines it.



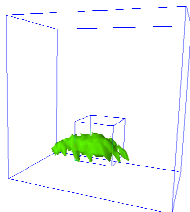
a) $\varepsilon_r^{(5,2)} = 3.9, n^{(5,2)} = 1.97$



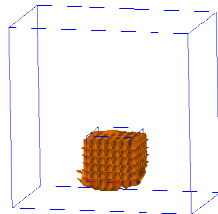
b) $\varepsilon_{r,h} \approx 4.2, n_{glob} = \sqrt{\varepsilon_{r,h}} \approx 2.05$

a) A sample of the reconstruction result of the dielectric cube No. 1 (4 cm side) via the first stage. b) Result after applying the adaptive stage (2-nd stage). The side of the cube is 4 cm=1.33 wavelength.

Results of the two-stage procedure, cube nr.2 (big)



a) $\epsilon_r(5,5) = 3.19, n^{(5,5)} = 1.79$



b) $\epsilon_{r,h} \approx 3.0, n_{glob} = \sqrt{\epsilon_{r,h}} \approx 1.73$

a) Reconstruction of the dielectric cube No. 2 (6 cm side) via the first stage. b) The final reconstruction result after applying the adaptive stage (2-nd stage). The side 6 cm=2 wavelength.

L.Beilina, M.V.Klibanov, Reconstruction of dielectrics from experimental data via a hybrid globally convergent/adaptive inverse algorithm, *Inverse Problems*, 26, 125009, 2010.

The Forward Problem in the approximate globally convergent method

$$\varepsilon_r(x)u_{tt} = \Delta u \text{ in } \mathbb{R}^3 \times (0, \infty), \quad (1)$$

$$u(x, 0) = 0, u_t(x, 0) = \delta(x - x_0). \quad (2)$$

$$\varepsilon_r(x) \in [1, d], d = \text{const.} > 1, \varepsilon_r(x) = 1 \text{ for } x \in \mathbb{R}^3 \setminus \Omega, \quad (3)$$

$$\varepsilon_r(x) \in C^2(\mathbb{R}^3). \quad (4)$$

- Applications: electromagnetic, acoustics

[RK] V. G. Romanov, M. V. Klibanov, CAN A SINGLE PDE GOVERN WELL THE PROPAGATION OF THE ELECTRIC WAVE FIELD IN A HETEROGENEOUS MEDIUM IN 3D?, <https://arxiv.org/abs/2102.02271>

Inverse Problem 1 (complete data)

Suppose that the coefficient $\varepsilon_r(x)$ satisfies (4) and (5), where the number $d > 1$ is given. Assume that the function $\varepsilon_r(x)$ is unknown in the domain Ω . Determine the function $\varepsilon_r(x)$ for $x \in \Omega$, assuming that the following function $g(x, t)$ is known for a single source position $x_0 \notin \overline{\Omega}$

$$u(x, t) = g(x, t), \forall (x, t) \in \partial\Omega \times (0, \infty). \quad (6)$$

- The function $g(x, t)$ in (6) is the result of measurement at the entire boundary.
- Uniqueness is known only if $\delta(x - x_0)$ is replaced with $f(x) \neq 0$ in $\overline{\Omega}$ (1981, the Bukhgeim-Klibanov method of Carleman estimates).
- Uniqueness theorem is a long standing open problem.
- We assume below that uniqueness holds true.

Definition of the Approximate Global Convergence Property

Definition (approximate global convergence)

- Consider a nonlinear ill-posed problem P . Suppose that this problem has a unique solution $x^* \in B$ for the noiseless data y^* , where B is a Banach space with the norm $\|\cdot\|_B$. We call x^* “exact solution” or “correct solution”.
- Suppose that a certain approximate mathematical model M_1 is proposed to solve the problem P numerically. Assume that, within the framework of the model M_1 , this problem has unique exact solution $x_{M_1}^*$. Also, let one of assumptions of the model M_1 be that $x_{M_1}^* = x^*$.
- Consider an iterative numerical method for solving the problem P . Suppose that this method produces a sequence of points $\{x_n\}_{n=1}^N \subset B$, where $N \in [1, \infty)$. Let the number $\varepsilon \in (0, 1)$.

Definition of the Approximate Global Convergence Property

We call this numerical method *approximately globally convergent of the level ε* , or shortly *globally convergent*, if, within the framework of the approximate model M_1 , a theorem is proven, which guarantees that, without any *a priori* knowledge of a sufficiently small neighborhood of x^* , there exists a number $\bar{N} \in [1, N)$ such that

$$\|x_n - x^*\|_B \leq \varepsilon, \forall n \geq \bar{N}. \quad (5)$$

Suppose that iterations are stopped at a certain number $k \geq \bar{N}$. Then the point x_k is denoted as $x_k := x_{glob}$ and is called “the approximate solution resulting from this method”.

The Approximately Globally Convergent Method

Laplace transform Consider the Laplace transform of the functions u in the hyperbolic equation (1),

$$w(x, s) = \int_0^{\infty} u(x, t) e^{-st} dt, \text{ for } s > \underline{s} = \text{const.} > 0, \quad (6)$$

where \underline{s} is a certain number. We assume that the number \underline{s} is sufficiently large and we call the parameter s *pseudo frequency*. Since $x_0 \notin \overline{\Omega}$ it follows from (1) and (78) that the function w is the solution of the following problem

$$\Delta w - s^2 \varepsilon_r(x) w = -\delta(x - x_0), \quad x \in \mathbb{R}^3, \quad (7)$$

$$\lim_{|x| \rightarrow \infty} w(x, s) = 0, \quad (8)$$

where limit in (8) is proved in [BK, Springer]. In [BK, Springer] was shown that $w(x, s) > 0$. Hence, we can consider functions $v(x, s)$ and $V(x, s)$ defined as

$$v(x, s) = \frac{\ln w(x, s)}{s^2}. \quad (9)$$

Lemma 1 (follows from a result of V.G. Romanov, 1984)

Suppose that the function $\varepsilon_r(x)$ satisfies conditions (4), (5). Assume that geodesic lines, generated by the eikonal equation corresponding to the function $\varepsilon_r(x)$ are regular. Then the following asymptotic behavior of the function w and its derivatives takes place for $|\beta| \leq 2, \gamma = 0, 1, x \neq x_0$

$$D_x^\beta D_s^\gamma w(x, s) = D_x^\beta D_s^\gamma \left\{ \frac{\exp[-sI(x, x_0)]}{f(x, x_0)} \left[1 + O\left(\frac{1}{s}\right) \right] \right\}, s \rightarrow \infty,$$

where $f(x, x_0)$ is a certain function and $f(x, x_0) \neq 0$ for $x \neq x_0$.

- Conditions of regularity of geodesic lines cannot be effectively verified. However, the entire theory of CIPs for hyperbolic PDEs does not work without this condition.
- We verify the asymptotic behavior computationally.

Assuming that the asymptotic behavior in Lemma 1 holds we get the following asymptotic behavior of the function v

$$\left\| D_x^\beta D_s^k v(x, s) \right\|_{C^3(\bar{\Omega})} = O\left(\frac{1}{s^{k+1}}\right), \quad s \rightarrow \infty, k = 0, 1. \quad (10)$$

Since the source $x_0 \notin \bar{\Omega}$, we obtain

$$\Delta v + s^2 (\nabla v)^2 = \varepsilon_r(x), \quad x \in \Omega. \quad (11)$$

The next step in our transformation procedure is to denote

$$q(x, s) = \partial_s v(x, s). \quad (12)$$

Using (10) and (12) we conclude that

$$v(x, s) = - \int_s^\infty q(x, \tau) d\tau.$$

The integral above can be rewritten also as

$$v(x, s) = - \int_s^{\bar{s}} q(x, \tau) d\tau + V(x, \bar{s}). \quad (13)$$

The function $V(x, \bar{s})$ in (13) is the “tail function” and such that

$$V(x, \bar{s}) = v(x, \bar{s}) = \frac{\ln w(x, \bar{s})}{\bar{s}^2}, \quad (14)$$

From (10) and (14) follows that

$$\|V(x, \bar{s})\|_{C^3(\bar{\Omega})} = O\left(\frac{1}{\bar{s}}\right), \quad \|\partial_{\bar{s}} V(x, \bar{s})\|_{C^3(\bar{\Omega})} = O\left(\frac{1}{\bar{s}^2}\right). \quad (15)$$

From (15) follows that the tail function is small for large values of \bar{s} . Therefore, one can set $V(x, \bar{s}) := 0$ or update the tail function in an iterative procedure.

The next step is differentiate (11) with respect to s . Using (12) and (13), we obtain the following nonlinear integral differential equation

$$\Delta q - 2s^2 \nabla q \int_s^{\bar{s}} \nabla q(x, \tau) d\tau + 2s \left[\int_s^{\bar{s}} \nabla q(x, \tau) d\tau \right]^2 + 2s^2 \nabla q \nabla V - 4s \nabla V \int_s^{\bar{s}} \nabla q(x, \tau) d\tau + 2s (\nabla V)^2 = 0, x \in \Omega. \quad (16)$$

(77) and (12) imply that the following Dirichlet boundary condition is given for the function q

$$q(x, s) = \psi(x, s), \quad \forall (x, s) \in \partial\Omega \times [s, \bar{s}], \quad (17)$$

where

$$\psi(x, s) = \frac{\partial_s \ln \varphi}{s^2} - \frac{2 \ln \varphi}{s^3} \quad (18)$$

and $\varphi(x, s)$ is the Laplace transform (78) of the known measured function $g(x, t)$.

New model of the tail function

Let the function $\varepsilon_r^*(x)$ satisfying to (2) be the exact solution of our **CIP** for the exact data g^* . Let $V^*(x, \bar{s})$ be the exact “tail function” defined as

$$V^*(x, \bar{s}) = \frac{\ln w^*(x, \bar{s})}{\bar{s}^2}. \quad (19)$$

Let $q^*(x, s) \in C^{2+\alpha}(\bar{\Omega}) \times C^1[\underline{s}, \bar{s}]$ and $\psi^*(x, s) \in C^{2+\alpha}(\bar{\Omega}) \times C^1[\underline{s}, \bar{s}]$ be the corresponding exact functions for q in (16) and ψ in (18). Then

$$\begin{aligned} \Delta q^* - 2s^2 \nabla q^* \cdot \int_s^{\bar{s}} \nabla q^*(x, \tau) d\tau + 2s \left[\int_s^{\bar{s}} \nabla q^*(x, \tau) d\tau \right]^2 + 2s^2 \nabla q^* \nabla V^* \\ - 2s \nabla V^* \cdot \int_s^{\bar{s}} \nabla q^*(x, \tau) d\tau + 2s (\nabla V^*)^2 = 0, \quad x \in \Omega, s \in [\underline{s}, \bar{s}], \\ q^*|_{\partial\Omega} = \psi^*(x, s) := \partial_s \varphi^*(x, s) \quad \forall (x, s) \in \partial\Omega \times [\underline{s}, \bar{s}]. \end{aligned} \quad (20)$$

Setting in (20) $s = \bar{s}$ we get following equation for functions q^* and V^*

$$\begin{aligned}\Delta q^* + 2\bar{s}^2 \nabla q^* \nabla V^* + 2\bar{s} (\nabla V^*)^2 &= 0, \quad x \in \Omega, \\ q^*|_{\partial\Omega} &= \psi^*(x, \bar{s}) \quad \forall x \in \partial\Omega.\end{aligned}\tag{21}$$

Next, we will assume that the exact functions $V^*(x, \bar{s}), q^*(x, \bar{s}), \bar{s} \rightarrow \infty$ have the following asymptotical behaviour

$$\begin{aligned}V^*(x, \bar{s}) &= \frac{p^*(x)}{\bar{s}} + O\left(\frac{1}{\bar{s}^2}\right) \approx \frac{p^*(x)}{\bar{s}}, \quad \bar{s} \rightarrow \infty, \\ q^*(x, \bar{s}) &= \partial_{\bar{s}} V^*(x, \bar{s}) = -\frac{p^*(x)}{\bar{s}^2} + O\left(\frac{1}{\bar{s}^3}\right) \approx -\frac{p^*(x)}{\bar{s}^2}, \quad \bar{s} \rightarrow \infty.\end{aligned}\tag{22}$$

Then, using the first terms in the asymptotic behavior (22) for the exact tail $V^*(x, \bar{s}) = \frac{p^*(x)}{\bar{s}}$ and for the exact function $q^*(x, \bar{s}) = -\frac{p^*(x)}{\bar{s}^2}$ we have

$$-\frac{\Delta p^*}{\bar{s}^2} - 2\bar{s}^2 \frac{\nabla p^*}{\bar{s}^2} \frac{\nabla p^*}{\bar{s}} + 2\bar{s} \frac{(\nabla p^*)^2}{\bar{s}^2} = 0, \quad x \in \Omega, \quad (23)$$

$$q^*|_{\partial\Omega} = \psi^*(x, \bar{s}) \quad \forall x \in \partial\Omega,$$

which is reduced to the following *approximate* Dirichlet boundary value problem for the function $p^*(x)$

$$\Delta p^* = 0 \text{ in } \Omega, \quad p^* \in C^{2+\alpha}(\bar{\Omega}), \quad (24)$$

$$p^*|_{\partial\Omega} = -\bar{s}^2 \psi^*(x, \bar{s}). \quad (25)$$

Approximate mathematical model

There exists a function $p^*(x) \in C^{2+\alpha}(\bar{\Omega})$ such that the exact tail function $V^*(x)$ has the form

$$V^*(x, s) := \frac{p^*(x)}{s}, \quad \forall s \geq \bar{s}. \quad (26)$$

Since $q^*(x, s) = \partial_s V^*(x, s)$ for $s \geq \bar{s}$, we can obtain from (26)

$$q^*(x, \bar{s}) = -\frac{p^*(x)}{\bar{s}^2}. \quad (27)$$

Then we can get following explicit formula for the reconstruction of the coefficient $\varepsilon_r^*(x)$

$$\varepsilon_r^*(x) = \Delta v^* + s^2 |\nabla v^*|^2,$$

where

$$v^* = - \int_s^{\bar{s}} q^*(x, \tau) d\tau + \frac{p^*(x)}{\bar{s}}.$$

Using the new mathematical model we will take the function

$$V_{1,0}(x) := \frac{p(x)}{\bar{s}}. \quad (28)$$

as the first guess for the tail function $V(x, \bar{s})$ where $p(x)$ is the solution of the problem following problem:

$$\Delta p = 0 \text{ in } \Omega, \quad p \in C^{2+\alpha}(\bar{\Omega}), \quad (29)$$

$$p|_{\partial\Omega} = -\bar{s}^2 \psi(x, \bar{s}). \quad (30)$$

The layer stripping procedure

Let us consider a layer stripping procedure with respect to the s by dividing the interval $[\underline{s}, \bar{s}]$ into N small subintervals of the step size $h = s_{n-1} - s_n$. Here,

$$\underline{s} = s_N < s_{N-1} < \dots < s_0 = \bar{s}. \quad (31)$$

The next step is to approximate the function $q(x, s)$ as a piecewise constant function with respect to s such that $q(x, s) = q_n(x)$ for $s \in [s_n, s_{n-1})$. Using (13) we can approximate value of the function $v(x, s_n)$ as

$$v(x, s_n) = -h \sum_{j=0}^n q_j(x) + V(x, \bar{s}), \quad q_0(x) \equiv 0. \quad (32)$$

Next, we introduce the s -dependent Carleman Weight Function (CWF)

$$C_{n,\mu}(s) = \exp[\mu(s - s_{n-1})], \quad (33)$$

where $\mu > 1$ is a large parameter.

We multiply both sides of equation (16) by $C_{n,\mu}(s)$ and integrate over pseudo-frequency to get the following system of equations on every pseudo-frequency interval (s_n, s_{n-1})

$$L_n(q_n) := \Delta q_n - A_{1,n} \left(h \sum_{j=0}^{n-1} \nabla q_j - \nabla V_n \right) \nabla q_n = B_n (\nabla q_n)^2 - A_{2,n} h^2 \left(\sum_{j=0}^{n-1} \nabla q_j \right)^2 + 2A_{2,n} \nabla V_n \left(h \sum_{j=0}^{n-1} \nabla q_j \right) - A_{2,n} (\nabla V_n)^2, \quad (34)$$

$$q_n|_{\partial\Omega} = \psi_n(x) := \frac{1}{h} \int_{s_n}^{s_{n-1}} \psi(x, s) ds, \quad n = 1, \dots, N.$$

Here integrals $A_{1,n}, A_{2,n}, B_n := \frac{l_{1,n}}{l_0}$ can be computed explicitly.

A finite element method for reconstruction

Once the functions V_n, q_n in (34) are calculated, we can compute the function $v_n(x)$ as

$$v_n(x) = -hq_n(x) - h \sum_{j=0}^{n-1} q_j(x) + V_n(x), \quad x \in \Omega. \quad (35)$$

Since

$$v_n(x) = \frac{\ln w_n(x, s_n)}{s_n^2}, \quad (36)$$

then $w_n(x) = \exp[s_n^2 v_n(x)]$ with known functions $v_n(x)$ on every pseudo-frequency interval (s_n, s_{n-1}) . Next, we apply the FEM to the equation (37) to obtain the function $\varepsilon_{r,n}$ with already computed w_n :

$$\Delta w_n - s_n^2 \varepsilon_{r,n}(x) w_n = 0 \text{ in } \Omega, \quad (37)$$

$$\partial_n w_n |_{\partial\Omega} = f_n(x), \quad (38)$$

where

$$f_n(x) = \partial_n \exp[s_n^2 v_n(x)] \text{ for } x \in \partial\Omega.$$

The finite element spaces

In computations we discretize our bounded domain $\Omega \subset \mathbb{R}^3$ by an unstructured tetrahedral mesh T using non-overlapping tetrahedral elements $K \in \mathbb{R}^3$. The elements K are such that $T = K_1, \dots, K_l$, where l is the total number of elements in Ω , and

$$\Omega = \cup_{K \in T} K = K_1 \cup K_2 \dots \cup K_l.$$

We associate with the mesh T the mesh function $h = h(x)$ as a piecewise-constant function such that

$$h(x) = h_K \quad \forall K \in T,$$

where h_K is the diameter of K which we define as the longest side of K . We make the following shape regularity assumption of the mesh T for every element $K \in T$

$$a_1 \leq h_K \leq r' a_2; \quad a_1, a_2 = \text{const.} > 0, \quad (39)$$

where r' is the radius of the maximal sphere contained in the element K .

We introduce now the finite element space V_h as

$$V_h = \{v(x) \in V : v \in C(\Omega), v|_K \in P_1(K) \forall K \in T\}, \quad (40)$$

where $P_1(K)$ denotes the set of piecewise-linear functions on K with

$$V = \{v(x) : v(x) \in H^1(\Omega)\}.$$

Hence, the finite element space V_h consists of continuous piecewise linear functions in space. The finite dimensional finite element space V_h is constructed such that $V_h \subset V$. To approximate functions $\varepsilon_{r,n}$ we introduce space of piecewise constants C_h defined by

$$C_h := \{u \in L_2(\Omega) : u|_K \in P_0(K), \forall K \in K_h\},$$

where $P_0(K)$ is the piecewise constant function defined in the vertices of the element K of the mesh K_h .

A finite element method

To compute $\varepsilon_{r,n}$ from (37), we will formulate the finite element method for the problem (37)-(38): Find $\varepsilon_{r,n} \in C_h$ for the known $w_n \in V_h$ such that $\forall v \in V_h$

$$(\varepsilon_{r,n} w_n, v) = -\frac{1}{s_n^2} (\nabla w_n, \nabla v) + \frac{1}{s_n^2} (f_n, v)_{\partial\Omega}. \quad (41)$$

We expand w_n in terms of the standard continuous piecewise linear functions $\{\varphi_k\}_{k=1}^N$ in space as

$$w_n = \sum_{k=1}^N w_{nk} \varphi_k(x),$$

where w_{nk} denote the nodal values of the function w_n at the nodes k of the mesh T . We can determine w_{nk} by knowing already computed functions $v_{n,k}$ using the formula

$$w_{nk} = \exp \left[s_n^2 v_{nk}(x) \right] \forall x \in \Omega.$$

We substitute this expansion in the variational formulation (41), choose $v(x) = \varphi_j(x)$ and obtain the following system of discrete equations

$$\sum_{k,j=1}^N \varepsilon_{r,nk} (w_{nk} \varphi_k, \varphi_j) = -\frac{1}{s_n^2} \sum_{k,j=1}^N w_{nk} (\nabla \varphi_k, \nabla \varphi_j) + \frac{1}{s_n^2} \sum_{j=1}^N (f_n, \varphi_j)_{\partial\Omega}. \quad (42)$$

The system (42) can be rewritten in the matrix form for the unknown $\varepsilon_{r,n} = \sum_{k=1}^N \varepsilon_{r,nk}$ and known w_n as

$$M \varepsilon_{r,n} = -\frac{1}{s_n^2} G w_n + \frac{1}{s_n^2} F. \quad (43)$$

Here, M is the block mass matrix in space, G is the stiffness matrix corresponding to the gradient term, F is the load vector. At the element level K the matrix entries in (43) are explicitly given by:

$$M_{k,j}^K = (w_{nk} \varphi_k, \varphi_j)_K, \quad (44)$$

$$G_{k,j}^K = (\nabla \varphi_k, \nabla \varphi_j)_K, \quad (45)$$

$$F_{n,j}^K = (f_n, \varphi_j)_K. \quad (46)$$

To obtain an explicit scheme for the computation of the coefficients $\varepsilon_{r,n}$, we approximate M by the lumped mass matrix M^L in space, i.e., the diagonal approximation obtained by taking the row sum of M , and get the following equation

$$\varepsilon_{r,n} = -\frac{1}{s_n^2}(M^L)^{-1}Gw_n + \frac{1}{s_n^2}(M^L)^{-1}F. \quad (47)$$

We note that for the case of linear Lagrange elements we have $M = M^L$ and thus, the lumping procedure does not include approximation errors in this case.

The Approximate Globally Convergent Algorithm

- Step 0** Compute the initial tail function $V_{n,0}(x, \bar{s}) \in C^{2+\alpha}(\bar{\Omega})$ as in (28).
- Step 1** Iterations (n, i) , $n, i \geq 1$. Solve the boundary value problem (33) and find function $q_{n,i}$.
- Step 2** Compute functions $v_{n,i}$ as

$$v_{n,i}(x) = -hq_{n,i} - h \sum_{j=0}^{n-1} q_j + V_{n,i}(x, \bar{s})$$

and then functions $w_{n,i}$ using

$$w_{n,i}(x) = \exp[s_n^2 v_{n,i}(x)].$$

- Step 3** Compute $\varepsilon_{r_{n,i}}$ via backwards calculations using the finite element formulation of the equation (37) as

$$\varepsilon_{r_{n,i}} = -\frac{1}{s_n^2} (M^L)^{-1} G w_{n,i} + \frac{1}{s_n^2} (M^L)^{-1} F,$$

where the matrices M , G and the vector F are defined on the element level $K \in T$ using (44) for $w_{n,i}$.

- Step 4** Solve the hyperbolic forward problem with computed $\varepsilon_{rn,i}$, and then compute the Laplace transform (78) to obtain $w_{n,i}$.
- Step 5** Find a new approximation for the tail function

$$V_{n,i}(x, \bar{s}) = \frac{\ln w_{n,i}(x, \bar{s})}{\bar{s}^2}.$$

- Step 6** Iterate with respect to i and stop iterations at $i = m_n$ such that $\varepsilon_{rn,m_n} := \lim_{i \rightarrow \infty} \varepsilon_{rn,i}$.
- Step 7** Set on the pseudo-frequency interval $[s_n, s_{n-1})$

$$q_n := q_{n,m_n}, \quad \varepsilon_{rn}(x) := \varepsilon_{rn,m_n}(x).$$

- Step 8** Stop computing functions ε_{rn} in the algorithm until functions ε_{rn} are converged. Else set $n = n + 1$, take new pseudo-frequency interval $[s_n, s_{n-1})$ for computations and go to step 1.

Approximate Global Convergence Theorem

(rough formulation) Let $\Omega \subset \mathbb{R}^3$ be a bounded domain with $\partial\Omega \in C^3$. Let the source $x_0 \notin \overline{\Omega}$. Let σ be the error in the boundary data,

$$\|\psi_n - \psi_n^*\|_{C^{2+\alpha}(\partial\Omega)} \leq C^* \sigma.$$

Consider the error parameter

$$\eta = 2(h + \sigma).$$

Let m be the maximal number of functions $q_{n,i}$ for each n and N be the maximal number of functions q_n :

$$\{q_{n,i}\}_{(i,n)=(1,1)}^{(m,N)}.$$

Introduce the set

$$P(d, d^*) = \left\{ c \in C^\alpha(\overline{\Omega}) : |c|_\alpha \leq d^* + \frac{1}{2}, c \in \left[1, d + \frac{1}{2}\right] \right\}.$$

Let the exact solution $c^* \in P(d, d^*)$, $c^* \in C^2(\mathbb{R}^3)$ for our CIP for $c^* u_{tt}^* - \Delta u^* = 0$.

Assume that all reconstructed functions $c_{n,i}(x) \geq 1$ in Ω . Let $\omega \in (0, 1)$ be a number. Then there exists a constant $B = B(\Omega, \bar{s}, d, d^*) > 2$ such that if the error ϵ is so small that

$$\epsilon \in \left(0, \frac{1}{B^{3Nm/\omega}}\right),$$

then all functions $c_{n,i} \in P(d, d^*) \cap C^\alpha(\bar{\Omega})$ and

$$\|c_{n,i} - c^*\|_{C^\alpha(\bar{\Omega})} \leq \epsilon^{1-\omega} := \theta \in (0, 1).$$

- The **DECISIVE ADVANTAGE** of this theorem is that it guarantees to provide a good approximation for the exact solution c^* without an a priori knowledge of a small neighborhood of c^* .
- Of course, this guarantee is valid only within the framework of the above approximate mathematical model.

QUESTION: Why a regularized solution of the Tikhonov functional is usually more accurate than the first guess for the practical case of a single value of the regularization parameter [1]? Indeed, the theory guarantees this only in the limiting case.

- One can improve the solution obtained in a globally convergent method
 - Adaptive approximately globally convergent algorithm [2].
 - Two-stage numerical procedure [3,4].
 - Relaxation property in the adaptivity [5].
1. M.V. Klibanov, A.B. Bakushinskii and L. Beilina, Why a minimizer of the Tikhonov functional is closer to the exact solution than the first guess? *J. Inverse and Ill-posed problems*, 19, pp.83-105, 2011
 2. M.Asadzadeh, L.Beilina, A posteriori error analysis in a globally convergent numerical method for a hyperbolic coefficient inverse problem, *Inverse Problems*, 26, 115007, 2010.
 3. L. Beilina and M.V. Klibanov, Synthesis of global convergence and adaptivity for a hyperbolic coefficient inverse problem in 3D, *J. Inverse and Ill-posed Problems*, 18, 85-132, 2010.
 4. L. Beilina and M.V. Klibanov, A posteriori error estimates for the adaptivity technique for the Tikhonov functional and global convergence for a coefficient inverse problem, *Inverse Problems*, 26, 045012, 2010.
 5. L. Beilina, M.V. Klibanov and M.Yu. Kokurin, Adaptivity with relaxation for ill-posed problems and global convergence for a coefficient inverse problem, *Journal of Mathematical Sciences*, 167, 279-325, 2010.

Relaxation property in the adaptivity

Theorem [BKK] Let $P_n : H_1 \rightarrow M_n$ be the orthogonal projection operator on the subspace M_n (a sequence of subspaces obtained via a mesh refinements). Assume that

$$x_{\alpha(\delta)} \neq P_n x_{\alpha(\delta)}$$

(otherwise, the regularized solution $x_{\alpha(\delta)}$ is found and belongs to the subspace M_n). Then there

$$\|x_n - x_\alpha\| \leq \theta_n \|x_{n-1} - x_\alpha\|, \theta_n \in (0, 1).$$

- Hence, [BKK, KBB]

$$\|x_n - x^*\| \leq \beta_n \|x_{n-1} - x_{\alpha(\delta)}\| + \xi \|x_{\alpha(\delta)} - x^*\|, \xi \in (0, 1).$$

L. Beilina, M.V. Klibanov and M.Yu. Kokurin, Adaptivity with relaxation for ill-posed problems and global convergence for a coefficient inverse problem, *Journal of Mathematical Sciences*, 167, 279-325, 2010.

M.V. Klibanov, A.B. Bakushinskii and L. Beilina, Why a minimizer of the Tikhonov functional is closer to the exact solution than the first guess? *J. Inverse and Ill-posed problems*, 19, pp.83-105, 2011.

First stage: experimental verification of a globally convergent method

- We use time-dependent experimental backscattered data measured at the Optoelectronics and Optical Communications Center at UNCC, USA.
- Our goal in experimental verification was to reconstruct different dielectric and metallic targets. For metallic targets we determine the effective or appearing dielectric constant such that

$$\varepsilon_r(\text{metal}) \in [10, 30]. \quad (48)$$

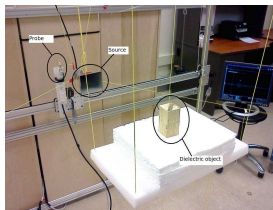
for metals. The set of admissible coefficients for the function $\varepsilon_r(\mathbf{x})$ in Ω is

$$M_{\varepsilon_r} = \{\varepsilon_r(\mathbf{x}) : \varepsilon_r(\mathbf{x}) \in [1, 25], \varepsilon_r(\mathbf{x}) = 1 \forall \mathbf{x} \in \mathbb{R}^3 \setminus \Omega.\}$$

- We compute refractive indexes n^{comp} of inclusions as

$$\varepsilon_r^{\text{comp}} = \max_{\bar{\Omega}} \varepsilon_r^{(\bar{N})}(x), n^{\text{comp}} = \sqrt{\varepsilon_r^{\text{comp}}}. \quad (49)$$

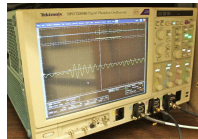
Data collection scheme



a)



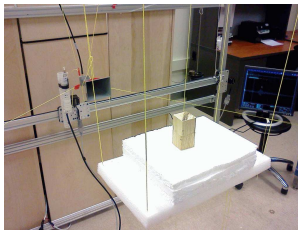
b)



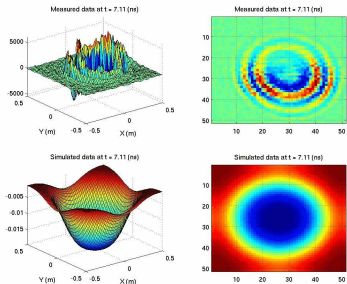
c)

Figure: a) A photograph explaining our data collection process. The distance between the target (wooden block) and the measurement plane is about 0.8 m, which is about 26 wave lengths. b) Picosecond Pulse Generator which generates electric pulses. It produced one component of the electrical field with the wavelength 0.03 meter every 10 picoseconds while tektronix oscilloscope registered backscattered data. The pulse goes to the transmitter which is a horn antenna (source). c) Detected signal is recorded by Tektronix Oscilloscope which produces a digitized time resolved signal with step size in time 10 picoseconds (10×10^{-12} sec.). The total time of measurements for one pulse is 10 nanoseconds (10×10^{-9} sec) = 10^4 picoseconds = 10^{-8} seconds which corresponds to 1000 timesteps.

Time-dependent data collection scheme



a)



b)

Figure: (a) Time-dependent data collection scheme using a picosecond pulse generator at the Optoelectronics Center of UNCC, Charlotte, USA. b) Spatial distribution of measured experimental versus simulated data for a metallic cylinder after application of the Laplace transform on the time-dependent data.

A mathematical model in imaging of targets

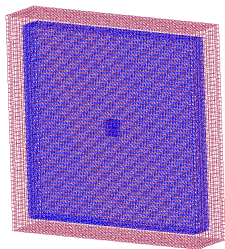
We choose the computational geometry Ω , see Figure 3. This geometry is split into two geometries, Ω_{FEM} and Ω_{FDM} such that $\Omega = \Omega_{FEM} \cup \Omega_{FDM}$. Next, we introduce dimensionless spatial variables $\mathbf{x}' = \mathbf{x} / (1\text{ m})$ and obtain that the domain Ω_{FEM} is transformed into our dimensionless computational domain

$$\Omega_{FEM} = \{\mathbf{x} = (x, y, z) \in (-0.5, 0.5) \times (-0.5, 0.5) \times (-0.1, 0.04)\}.$$

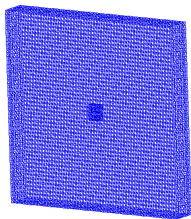
To compute tail functions in an approximate globally convergent algorithm, we solve the forward problem using the software package WavES (waves24.com) via the hybrid FEM/FDM method [BSA]. The dimensionless size of our computational domain Ω for the forward problem is

$$\Omega = \{\mathbf{x} = (x, y, z) \in (-0.56, 0.56) \times (-0.56, 0.56) \times (-0.16, 0.1)\}.$$

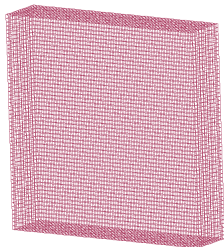
Hybrid FEM/FDM geometry



a)



b)



c

Figure: a) Hybrid FEM/FDM geometry Ω ; b) Ω_{FEM} ; c) Ω_{FDM} .

We use the hybrid method of [BSA] since we know $\varepsilon_r(\mathbf{x}) = 1$ in Ω_{FDM} and we need to determine $\varepsilon_r(\mathbf{x})$ only in Ω_{FEM} . The forward problem in our tests is

$$\begin{aligned}
 \varepsilon_r(\mathbf{x}) u_{tt} - \Delta u &= 0, & \text{in } \Omega \times (0, T), \\
 u(\mathbf{x}, 0) = 0, u_t(\mathbf{x}, 0) &= 0, & \text{in } \Omega, \\
 u &= f(t), & \text{on } \partial\Omega_1 \times (0, t_1], \\
 \partial_n u &= -\partial_t u, & \text{on } \partial\Omega_1 \times (t_1, T), \\
 \partial_n u &= -\partial_t u, & \text{on } \partial\Omega_2 \times (0, T), \\
 \partial_n u &= 0, & \text{on } \partial\Omega_3 \times (0, T),
 \end{aligned} \tag{50}$$

where $f(t)$ is initialized plane wave,

$$f(t) = \sin \omega t, \quad 0 \leq t \leq t_1 := \frac{2\pi}{\omega}. \tag{51}$$

$\partial\Omega_1$ - backscattering boundary, $\partial\Omega_2$ - transmitted boundary,

$$\partial\Omega_3 = \partial\Omega \setminus \partial\Omega_1 \cup \partial\Omega_2.$$

[BSA]L. Beilina, K. Samuelsson and K. Åhlander, Efficiency of a hybrid method for the wave equation. In *International Conference on Finite Element Methods*, Gakuto International Series Mathematical Sciences and Applications, Gakkotosho CO., LTD, 2001.

Boundary conditions and the choice of the s -interval

To solve uniquely the equations (34) on every pseudo-frequency interval it is necessary to know the function $u(x, t) := g(x, t)$ at the entire boundary Γ . However, our backscattering data are given only on the part Γ_1 of the domain Ω_{FEM} . Our observations provide a numerical justification for assigning the following boundary condition at Γ :

$$w(x, s) |_{\Gamma} = \begin{cases} w_T(x, s), & x \in \Gamma_1, \\ w_{unif}(x, s), & x \in \Gamma \setminus \Gamma_1. \end{cases} \quad (52)$$

Here $w_T(x, s)$ is the Laplace transform (78) of the total field $u_T(x, t)$, and $w_{unif}(x, s)$ is the the Laplace transform of the solution of (50) for the uniform medium with $\varepsilon_r(\mathbf{x}) = 1$.

We take the following s - interval

$$s \in [8, 10], h = 0.05, \quad (53)$$

where $h = s_{n-1} - s_n$ is step in pseudo-frequency.

Object number	Name of the object
1	a piece of oak
2	a piece of pine
3	a metallic sphere
4	a metallic cylinder
5	blind target
6	blind target
7	blind target
8	doll, air inside, blind target
9	doll, metal inside, blind target
10	doll, sand inside, blind target
11	two metallic blind targets

Table: *Object names.*

Backscattered experimental data, objects 1, 2

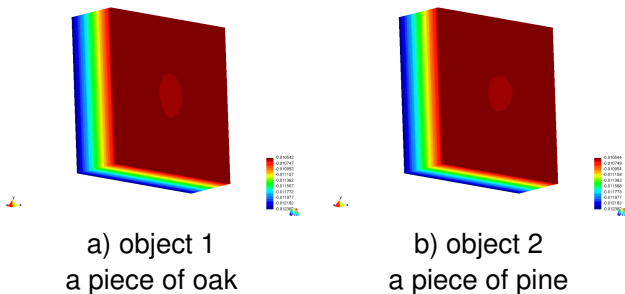


Figure: Test 1. Backscattered experimental data $\psi(x, s)$, $x \in \Gamma_1$ immersed into data $\psi(x, s)$, $x \in \Gamma \setminus \Gamma_1$ computed with $\varepsilon_r(x) = 1$ in Ω_{FEM} at pseudo-frequency $s = 9.2$.

Backscattered experimental data

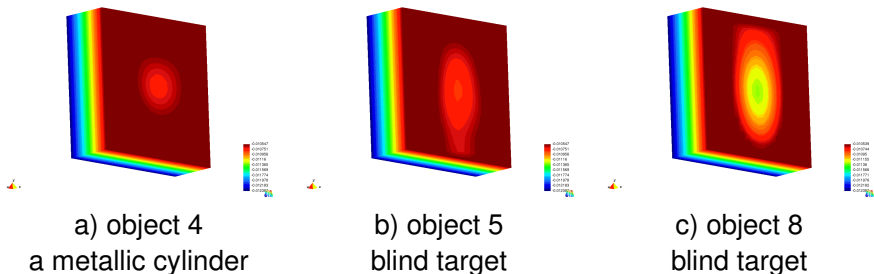


Figure: Test 1. Backscattered experimental data $\psi(x, s)$, $x \in \Gamma_1$ immersed into data $\psi(x, s)$, $x \in \Gamma \setminus \Gamma_1$ computed with $\varepsilon_r(x) = 1$ in Ω_{FEM} at pseudo-frequency $s = 9.2$.

Two main steps are:

- Data propagation: we used the time-reversal method to propagate the measured scattered waves from the measurement plane to the plane which was at only about 4 cm from the targets.
- Data calibration: to scale the measured data to the same scaling as in our simulations. This was done by using calibrating objects. We calibrated the non-metallic and metallic targets differently. We assumed that we know object1 (non-metallic) and object4 (metallic). We simulated the data for these two targets. Then we multiplied our measured data by the ratio between the simulated and measured data of our calibrating objects.

Nguyen Trung Thành, L. Beilina, M. V. Klibanov and M. A. Fiddy, Reconstruction of the refractive index from experimental backscattering data using a globally convergent inverse method, *SIAM J. Scientific Computing*, accepted for publication; preprint: *arXiv* :1306.3150 [math-ph], 2013.

Results of experiments of the first stage

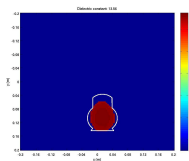
Target number	1	2	5	8	10	Average error
blind/non-blind (yes/no)	no	no	yes	yes	yes	
Measured n , error	2.11, 19%	1.84, 18%	2.14, 28%	1.89, 30%	2.1, 26%	24%
n^{comp} of Test 1, error	1.92, 10%	1.8, 2%	1.83, 17%	1.86, 2%	1.92, 9%	8%
n^{comp} of Test 2, error	2.07, 2%	2.01, 10%	2.21, 3%	1.83, 3%	2.2, 5%	4.6%
n^{comp} of Test 3, error	2.017, 5%	2.013, 9%	2.03, 5%	1.97, 4%	2.02, 4%	5%

Table: Computed n^{comp} and directly measured refractive indices of dielectric targets together with both measurement and computational errors as well as the average error. Note that the average computing errors are at least three times less than the average error of direct measurements.

Target number	3	4	6	7	9	11
blind/non-blind (yes/no)	no	no	yes	yes	yes	yes
ϵ_r^{comp} of Test 1	14.4	15.0	15	13.6	13.6	13.1
ϵ_r^{comp} of Test 2	15	15	15	14.1	14.1	15
ϵ_r^{comp} of Test 3	15	15	15	15	14	14.06

Table: Computed appearing dielectric constants ϵ_r^{comp} of metallic targets number 3,4,6,7,11 as well as of the target number 9 which is a metal covered by a dielectric.

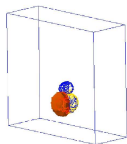
Reconstructed results of wooden doll and metallic block inside



a) estimated xy sizes



b) front view



c) 3D view



d) side view

Figure: Reconstructed “apparent” $\varepsilon(x) \approx 13.56$ on the mesh with the mesh size $h=0.02$

Second stage: adaptive finite element method

We use the following model problem for the electric field E with the stabilizing divergence condition with $s \geq 1$:

$$\varepsilon_r \frac{\partial^2 E}{\partial t^2} + \nabla \times (\nabla \times E) - s \nabla (\nabla \cdot (\varepsilon_r E)) = 0, \text{ in } \Omega_T, \quad (54)$$

$$E(\mathbf{x}, 0) = 0, \quad E_t(\mathbf{x}, 0) = 0 \text{ in } \Omega. \quad (55)$$

We impose the following boundary conditions

$$E(\mathbf{x}, t) = (0, f(t), 0) \text{ on } \partial_2 \Omega \times (0, t_1], \quad (56)$$

$$\partial_n E(\mathbf{x}, t) = -\partial_t E(\mathbf{x}, t) \text{ on } \partial_1 \Omega \times (t_1, T), \quad (57)$$

$$\partial_n E(\mathbf{x}, t) = -\partial_t E(\mathbf{x}, t) \text{ on } \partial_2 \Omega_T, \quad (58)$$

$$\partial_n E(\mathbf{x}, t) = 0 \text{ on } \partial_3 \Omega_T, \quad (59)$$

where ∂_n is the normal derivative.

Using the transformation $\nabla \times (\nabla \times E) = \nabla(\nabla \cdot E) - \nabla \cdot (\nabla E)$, the model problem (54), (55), (56) – (59) can be rewritten as

$$\varepsilon_r \frac{\partial^2 E}{\partial t^2} + \nabla(\nabla \cdot E) - \nabla \cdot (\nabla E) - s \nabla(\nabla \cdot (\varepsilon_r E)) = 0, \text{ in } \Omega_T, \quad (60)$$

$$E(\mathbf{x}, 0) = 0, \quad E_t(\mathbf{x}, 0) = 0 \text{ in } \Omega, \quad (61)$$

with boundary conditions

$$E(\mathbf{x}, t) = (0, f(t), 0) \text{ on } \partial_1 \Omega \times (0, t_1], \quad (62)$$

$$\partial_n E(\mathbf{x}, t) = -\partial_t E(\mathbf{x}, t) \text{ on } \partial_1 \Omega \times (t_1, T), \quad (63)$$

$$\partial_n E(\mathbf{x}, t) = -\partial_t E(\mathbf{x}, t) \text{ on } \partial_2 \Omega_T, \quad (64)$$

$$\partial_n E(\mathbf{x}, t) = 0 \text{ on } \partial_3 \Omega_T. \quad (65)$$

Tikhonov functional and optimality conditions

Our goal is to find ε_r by minimizing the Tikhonov functional:

$$F(\varepsilon_r) = F(E, \varepsilon_r) := \frac{1}{2} \int_{S_T} (E - \tilde{g})^2 z_\delta(t) d\mathbf{x} dt + \frac{1}{2} \gamma \int_G (\varepsilon_r - \varepsilon_{r, glob})^2 d\mathbf{x}, \quad (66)$$

where $\gamma > 0$ is the regularization parameter, and $\varepsilon_{r, glob}(\mathbf{x})$ is the computed coefficient via the globally convergent method.

Minimization is performed via Lagrangian

$$L(E, \lambda, \varepsilon_r) = F(E, \varepsilon_r) + \int_{\Omega_T} \lambda \left(\varepsilon_r \frac{\partial^2 E}{\partial t^2} + \nabla(\nabla \cdot E) - \nabla \cdot (\nabla E) - s \nabla(\nabla \cdot (\varepsilon_r E)) \right) d\mathbf{x} dt.$$

Then we search for a stationary point $w \in U^1$ such that

$$L'(w)(\bar{w}) = 0, \quad \forall \bar{w} \in U^1, \quad (67)$$

$$U^1 = H_E^1(\Omega_T) \times H_\lambda^1(\Omega_T) \times B(\Omega),$$

where $B(\Omega)$ is the space of functions bounded on Ω with the norm $\|f\|_{B(\Omega)} = \sup_\Omega |f|$. To find the Fréchet derivative $L'(w)$, we consider

$L(w + \bar{w}) - L(w)$, $\forall \bar{w} \in U^1$ and single out the linear, with respect to \bar{w} , part to get for $\mathbf{x} \in \Omega$

$$L'(w)(\mathbf{x}) = \gamma (\varepsilon_r - \varepsilon_{r, glob})(\mathbf{x}) - \int_0^T \frac{\partial \lambda}{\partial t} \frac{\partial E}{\partial t}(\mathbf{x}, t) dt + s \int_0^T (\nabla \cdot E)(\nabla \cdot \lambda)(\mathbf{x}, t) dt. \quad (68)$$

The adjoint problem

The adjoint problem is:

$$\begin{aligned}\varepsilon_r \frac{\partial^2 \lambda}{\partial t^2} + \nabla(\nabla \cdot \lambda) - \nabla \cdot (\nabla \lambda) - \mathbf{s} \varepsilon_r \nabla(\nabla \cdot \lambda) &= 0, \text{ in } \Omega_T, \\ \lambda(\mathbf{x}, T) = 0, \quad \lambda_t(\mathbf{x}, T) &= 0 \text{ in } \Omega_T, \\ \partial_n \lambda(\mathbf{x}, t) &= z_\delta(t) (\tilde{\mathbf{g}} - E)(\mathbf{x}, t) \text{ on } S_T.\end{aligned}\tag{69}$$

Here, $z_\delta(t)$ is used to ensure the compatibility conditions at $\overline{Q}_T \cap \{t = T\}$ for the adjoint problem and $\delta > 0$ is a small number.

The finite element discretization

Consider a partition $K_h = \{K\}$ of Ω_{FEM} which consists of tetrahedra with a mesh function h defined as $h|_K = h_K$ — the local diameter of the element K . Let $J_\tau = \{J\}$ be a partition of the time interval $(0, T)$ into subintervals $J = (t_{k-1}, t_k]$ of uniform length $\tau = t_k - t_{k-1}$. We also assume the minimal angle condition on the K_h .

We define the finite element spaces $V_h \subset L_2(\Omega_{FEM})$, $W_h^E \subset H_E^1(\Omega_{FEMT})$ and $W_h^\lambda \subset H_\lambda^1(\Omega_{FEMT})$, $\Omega_{FEMT} = \Omega_{FEM} \times (0, T)$, such that

$$W_h^E := \{w \in H_E^1 : w|_{K \times J} \in P_1(K) \times P_1(J), \forall K \in K_h, \forall J \in J_\tau\},$$

where $P_1(K)$ and $P_1(J)$ denote the set of linear functions on K and J , respectively. We also introduce the finite element test space W_h^λ defined by

$$W_h^\lambda := \{w \in H_\lambda^1 : w|_{K \times J} \in P_1(K) \times P_1(J), \forall K \in K_h, \forall J \in J_\tau\}.$$

Hence, the finite element spaces W_h^E and W_h^λ consist of continuous piecewise linear functions in space and time. To approximate the function $\varepsilon_r(\mathbf{x})$, we use the space of piecewise constant functions $V_h \subset L_2(\Omega_{FEM})$,

$$V_h := \{u \in L_2(\Omega_{FEM}) : u|_K \in P_0(K), \forall K \in K_h\}, \quad (70)$$

where $P_0(K)$ is the set of piecewise constant functions on K .

We also compute

$$\bar{\varepsilon}_r(\mathbf{x}) = \begin{cases} \varepsilon_r(\mathbf{x}), & \mathbf{x} \in \Omega_{FEM}, \\ 1, & \mathbf{x} \in \Omega_{FDM}. \end{cases} \quad (71)$$

Next, we set $U_h = W_h^E \times W_h^\lambda \times V_h$. Obviously $\dim U_h < \infty$ and $U_h \subset U^1$ as a set. Because of this, we consider U_h as a discrete analogue of the space U^1 . We introduce the same norm in U_h as the one in U^0 , $\|\cdot\|_{U_h} := \|\cdot\|_{U^0}$, with

$$U^0 = L_2(G_T) \times L_2(G_T) \times L_2(\Omega).$$

The finite element method for solving equation (67) now reads: *Find $u_h \in U_h$, such that*

$$L'(u_h)(\bar{u}) = 0, \quad \forall \bar{u} \in U_h. \quad (72)$$

General framework for a posteriori error estimation for CIPs

We present a posteriori error estimate for three kinds of error:

- For the error $|L(u) - L(u_h)|$ in the Lagrangian with $u = (E, \lambda, \varepsilon_r)$, $u_h = (E_h, \lambda_h, \varepsilon_h)$ [BJ1, B, BJ2].
- For the error $|F(\varepsilon_r) - F(\varepsilon_h)|$ in the Tikhonov functional [BK].
- For the error $|\varepsilon_r - \varepsilon_h|$ in the regularized solution of this functional ε_r [BK].

To achieve the first and the second goals, we note that

$$\begin{aligned}L(u) - L(u_h) &= L'(u_h)(u - u_h) + R(u, u_h), \\F(\varepsilon_r) - F(\varepsilon_h) &= F'(\varepsilon_h)(\varepsilon_r - \varepsilon_h) + R(\varepsilon_r, \varepsilon_h),\end{aligned}\tag{73}$$

where $R(u, u_h)$, $R(\varepsilon_r, \varepsilon_h)$ are the second order remainders terms. We assume that ε_h is located in the small neighborhood of the regularized solution ε_r . Thus, the terms $R(u, u_h)$, $R(\varepsilon_r, \varepsilon_h)$ are small and we can neglect them.

[BJ1] L. Beilina and C. Johnson, A hybrid FEM/FDM method for an inverse scattering problem. In *Numerical Mathematics and Advanced Applications, ENUMATH 2001*, Springer-Verlag, Berlin, 2001.

[B] Beilina, Adaptive hybrid FEM/FDM methods for inverse scattering problems, *Inverse problems and information technologies*, 1 (2), 73-116, 2002.

We now use the Galerkin orthogonality principle

$$\begin{aligned}L'(u_h)(\bar{u}) &= 0 \quad \forall \bar{u} \in U_h, \\F'(\varepsilon_h)(b) &= 0 \quad \forall b \in V_h,\end{aligned}\tag{74}$$

together with the splitting

$$\begin{aligned}u - u_h &= (u - u_h^I) + (u_h^I - u_h), \\ \varepsilon_r - \varepsilon_h &= (\varepsilon_r - \varepsilon_h^I) + (\varepsilon_h^I - \varepsilon_h),\end{aligned}\tag{75}$$

where $u_h^I \in U_h$ is the interpolant of u , and $\varepsilon_h^I \in V_h$ is the interpolant of ε_r , and get the following error representation:

$$\begin{aligned}L(u) - L(u_h) &\approx L'(u_h)(u - u_h^I), \\ F(\varepsilon_r) - F(\varepsilon_h) &\approx F'(\varepsilon_h)(\varepsilon_r - \varepsilon_h^I).\end{aligned}\tag{76}$$

In a posteriori error estimate (76)

- Terms $L'(u_h)$ and $F'(\varepsilon_h)$ represents residuals.
- Terms $u - u_h^I$ and $\varepsilon_r - \varepsilon_h^I$ are weights.

Interpolation property and estimation of weights

Let M be a subspace of the space V . Let $P_h : V \rightarrow M$ for $\forall M \subset V$, be the operator of the orthogonal projection of V on M . Let the function $f \in H^1(\Omega) \cap C(\Omega)$ and $\partial_{x_i} f_{x_i} \in L_\infty(\Omega)$. We define by f_k^I the standard interpolant [EEJ, JS] on triangles/tetrahedra of the function $f \in H$. Then by one of properties of the orthogonal projection

$$\|f - P_h f\|_{L_2(\Omega)} \leq \|f - f_k^I\|_{L_2(\Omega)}. \quad (77)$$

It follows from [EEJ] that

$$\|f - P_h f\|_{L_2(\Omega)} \leq C_I \|h \nabla f\|_{L_2(\Omega)}, \quad \forall f \in V. \quad (78)$$

where $C_I = C_I(\Omega)$ is positive constant depending only on the domain Ω and the mesh function $h = h(x)$ is a piecewise-constant function such that

$$h(x) = h_K \quad \forall K \in T,$$

where h_K is the diameter of K which we define as the longest side of K . In addition, we can estimate [JS]

$$|\nabla f| \leq \frac{|[f_h]|}{h_K}.$$

To derive the error $\varepsilon_r - \varepsilon_h$ in the regularized solution ε_r we use the convexity property of the Tikhonov functional together with the interpolation property (78).

Theorem [BKBook] *Let $z_h \in V_h$ be a finite element approximation of the regularized solution $z_\alpha \in H^1(\Omega)$ on the finite element mesh T with the mesh function h . Then there exists a constant D such that*

$\|F'(z_1) - F'(z_2)\| \leq D \|z_1 - z_2\|, \forall z_1, z_2 \in H$ such that the following a posteriori error estimate for the regularized solution z_α holds

$$\|z_h - z_\alpha\|_{L^2(\Omega)} \leq \frac{D}{\alpha} C_I \|hz_h\|_{L_2(\Omega)}.$$

From Theorem 5.1 and Remark 5.1 of [LB] it follows that the finite element mesh should be locally refined in such subdomain of Ω_{FEM} where the maximum norm of the Fréchet derivative of the objective functional is large. We always interpolate the initial approximation $\varepsilon_{r, glob}$ from the previous mesh to the new mesh. Denote by

$$L'_h{}^m(\mathbf{x}) = - \int_0^T \frac{\partial \lambda_h^m}{\partial t} \frac{\partial E_h^m}{\partial t} dt + s \int_0^T \nabla \cdot E_h^m \nabla \cdot \lambda_h^m dt + \gamma(\bar{\varepsilon}_h^m - \bar{\varepsilon}_{r, glob}). \quad (79)$$

[LB] L. Beilina, Adaptive Finite Element Method for a coefficient inverse problem for the Maxwell's system, *Applicable Analysis*, 90, 1461-1479, 2011.

[BKBook] L. Beilina and M.V. Klibanov, *Approximate Global Convergence and Adaptivity for Coefficient Inverse Problems*, Springer, New York, 2012.

Adaptive algorithm

- Step 0.** Choose an initial mesh K_h in Ω and an initial time partition J_0 of the time interval $(0, T)$. Start from the initial guess $\varepsilon_h^0 = \varepsilon_{r, glob}$, we compute the approximations ε_h^m via the following steps:
- Step 1.** Compute the solutions $E_h(x, t, \varepsilon_h^m)$ and $\lambda_h(x, t, \varepsilon_h^m)$ of the state problem and the adjoint problem on K_h and J_k , and compute the Fréchet derivative $L_h^{\prime, m}$ via (79).
- Step 2.** Update the coefficient on K_h and J_k using the conjugate gradient method:

$$\varepsilon_h^{m+1} := \varepsilon_h^m + \alpha d^m(\mathbf{x}),$$

where $\alpha > 0$ is a step-size in the conjugate gradient method and

$$d^m(\mathbf{x}) = -L_h^{\prime, m}(\mathbf{x}) + \beta^m d^{m-1}(\mathbf{x}),$$

with

$$\beta^m = \frac{\|L_h^{\prime, m}\|^2}{\|L_h^{\prime, m-1}\|^2},$$

where $d^0(\mathbf{x}) = -L_h^{\prime, 0}(\mathbf{x})$.

- Step 3.** Stop updating the coefficient and set $\varepsilon_h := \varepsilon_h^{m+1}$, $M := m + 1$, if either $\|L_h^{\prime, m}\|_{L_2(\Omega)} \leq \theta$ or norms $\|\varepsilon_h^m\|_{L_2(\Omega)}$ are stabilized. Here θ is a tolerance number. Otherwise, set $m := m + 1$ and go to step 1.
- Step 4.** Compute $L_h^{\prime, M}$ via (79). Refine the mesh at all grid points \mathbf{x} where

$$|L_h^{\prime, M}(\mathbf{x})| \geq \beta_1 \max_{\Omega} |L_h^{\prime, M}(\mathbf{x})|. \quad (80)$$

Here the tolerance number $\beta_1 \in (0, 1)$ is chosen by the user.

- Step 5.** Construct a new mesh K_h and a new time partition J_k such that the CFL condition is satisfied. Return to step 1 at $m = 1$ and perform all above steps on the new mesh. Stop mesh refinements if norms defined in step 3 either increase or stabilize, compared with the previous mesh.

Names of targets

Target number	Specification of the target
1	a piece of oak, rectangular prism
2	a piece of pine
3	a metallic sphere
4	a metallic cylinder
5	a piece of oak
6	a metallic rectangular prism
7	a wooden doll, air inside, heterogeneous target
8	a wooden doll, metal inside, heterogeneous target
9	a wooden doll, sand inside, heterogeneous target

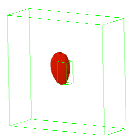
Target number	1	2	5	7	9	Average error
Measured n , error	2.11, 19%	1.84, 18%	2.14, 28%	1.89, 30%	2.1, 26%	24%
n in glob.conv, error	1.92, 9%	1.8, 2%	1.83, 15%	1.86, 2%	1.92, 9%	8%
n , coarse mesh, error	1.94, 8%	1.82, 1%	1.84, 14%	1.88, 0.5%	1.93, 8%	6%
n , 1 time ref. mesh, error	1.94, 8%	1.82, 1%	1.85, 14 %	1.89, 0%	1.93, 8%	6%
n , 2 times ref.mesh, error		1.84, 0%		1.9, 0.5%	1.96, 7%	2%
n , 3 times ref.mesh, error				1.89,0 %		0%

Table: Computed $n(\text{target})$ and directly measured refractive indices of dielectric targets together with both measurement and computational errors as well as the average error.

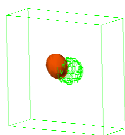
Target number	3	4	6	8
$\epsilon_r(\text{target})$ of glob.conv.	14.4	15.0	25	13.6
$\epsilon_r(\text{target})$ coarse mesh	14.4	17.0	25	13.6
$\epsilon_r(\text{target})$ 1 time ref.mesh	14.5	17.0	25	13.6
$\epsilon_r(\text{target})$ 2 times ref.mesh	14.6	17.0	25	13.7
$\epsilon_r(\text{target})$ 3 times ref.mesh	14.6	17.0		14.0
$\epsilon_r(\text{target})$ 4 times ref.mesh		17.0		

Table: Computed appearing dielectric constants $\epsilon_r(\text{target})$ of metallic targets with numbers 3,4,6 as well as of target number 8 which is a metal covered by a dielectric.

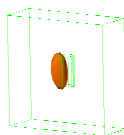
Initial guesses obtained on the first stage



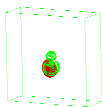
a) target 1



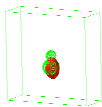
b) target 3



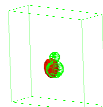
c) target 4



d) target 7



e) target 8



f) target 9

Figure: Reconstructions of some targets obtained on the first stage of our two-stage numerical procedure.

Reconstruction of a piece of oak

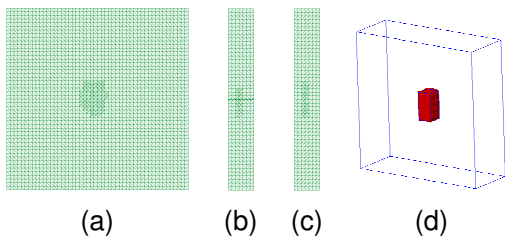
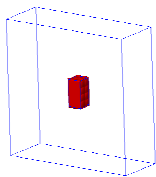
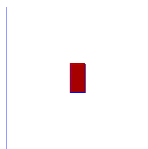


Figure: (a) xy -projection, (b) xz -projection, and (c) yz -projection of the once refined (optimal) mesh; d) Computed image of target 1 (a piece of oak) on that mesh. Thin lines indicate correct shapes.

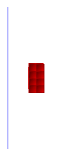
Reconstruction of a piece of oak



(a) Perspective view



(b) Front view



(c) Side view



(d) Zoom, perspective



(e) Zoom, front



(f) Zoom, side

Figure: Three views and zooms of the reconstruction of target number 1 (a piece of oak) (figures a)-f)) on the once refined mesh.

Reconstruction of a metallic sphere

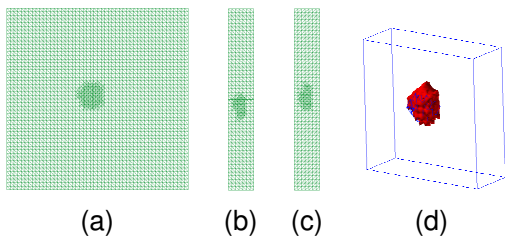
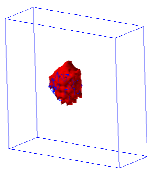
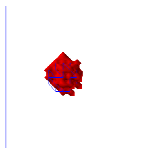


Figure: (a) xy -projection, (b) xz -projection, and (c) yz -projection of the three times refined (optimal) mesh; (d) Computed image of target number 3 (a metallic sphere) on that mesh. Thin lines indicate correct shape.

Reconstruction of a metallic sphere



(g) Perspective view



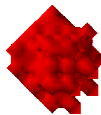
(h) Front view



(i) Side view



(j) Zoom, perspective



(k) Zoom, front



(l) Zoom, side

Figure: Three views and zooms of the reconstruction of target number 3 (figures g)-l), a metallic sphere) on three times refined mesh.

Reconstruction of a wooden doll, air inside

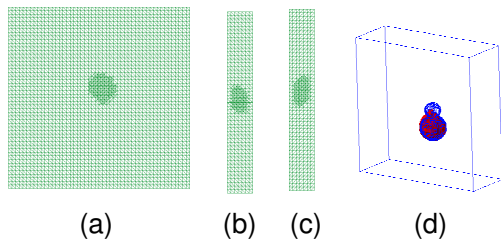
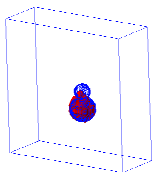
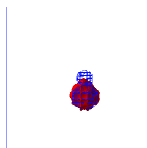


Figure: (a) xy -projection, (b) xz -projection, and (c) yz -projection of the three times refined (optimal) mesh; (d) Computed image of target number 7 (doll, air inside) on that mesh. Thin lines indicate correct shape.

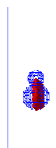
Reconstruction of a wooden doll, air inside



(a) Perspective view



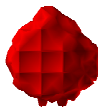
(b) Front view



(c) Side view



(d) Zoom, perspective



(e) Zoom, front



(f) Zoom, side

Figure: Three views and zooms of targets number 7 (figures a)-f), doll, air inside) on three times refined mesh. Thin lines indicate correct shape.

Reconstruction of a wooden doll, metal inside

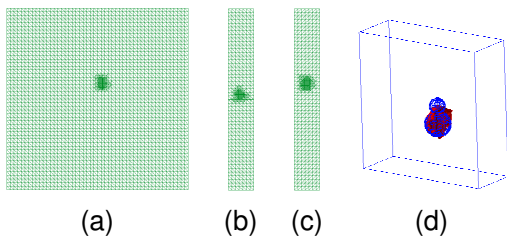
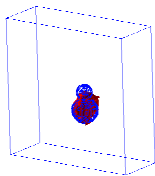


Figure: (a) xy -projection, (b) xz -projection, and (c) yz -projection of the three times refined (optimal) mesh and the reconstruction (d) of target number 8 (doll, metal inside) on the optimal mesh.

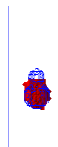
Reconstruction of a wooden doll, metal inside



(g) Perspective view



(h) Front view



(i) Side view



(j) Zoom, perspective



(k) Zoom, front



(l) Zoom, side

Figure: Three views and zooms of targets number 8 (figures g)-l), doll, metal inside) on three times refined mesh.

Reconstruction of a wooden doll, sand inside

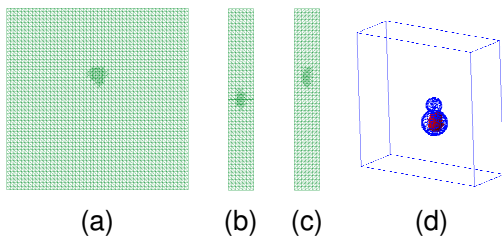
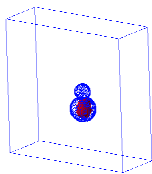
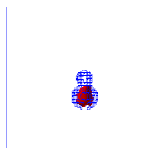


Figure: (a) xy -projection, (b) xz -projection, and (c) yz -projection of the twice refined (optimal) mesh and the reconstruction (d) of target number 9 (doll, sand inside) on the three times refined mesh.

Reconstruction of a wooden doll, sand inside



(a) Perspective view



(b) Front view



(c) Side view



(d) Zoom, perspective



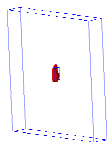
(e) Zoom, front



(f) Zoom, side

Figure: Three views and zooms of target number 9 (doll, sand inside) on twice refined mesh. Thin lines indicate correct shape.

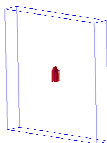
Dynamics of reconstruction of a metallic cylinder on a locally refined meshes



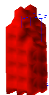
a) once refined



b) zoom



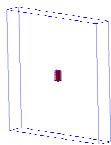
c) twice refined



d) zoom

Figure: Computed images of target number 4 (a metallic cylinder).

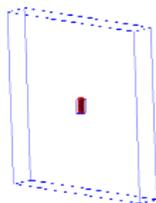
Dynamics of reconstruction of a metallic cylinder on a locally refined meshes



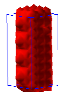
a) three times refined



b) zoom



c) four times refined



d) zoom

Figure: Computed images of target number 4 (a metallic cylinder).

References

- L. Beilina and C. Johnson, A posteriori error estimation in computational inverse scattering, *Mathematical Models in Applied Sciences*, 1, 23-35, 2005.
- L. Beilina and M.V. Klibanov, A globally convergent numerical method for a coefficient inverse problem, *SIAM J. Sci. Comp.*, 31, 478-509, 2008.
- M.Asadzadeh, L.Beilina, A posteriori error analysis in a globally convergent numerical method for a hyperbolic coefficient inverse problem, *Inverse Problems*, 26, 115007, 2010.
- L. Beilina and M.V. Klibanov, Synthesis of global convergence and adaptivity for a hyperbolic coefficient inverse problem in 3D, *J. Inverse and Ill-posed Problems*, 18, 85-132, 2010.
- L. Beilina and M.V.Klibanov, Reconstruction of dielectrics from experimental data via a hybrid globally convergent/adaptive inverse algorithm, *Inverse Problems*, 26, 125009, 2010. Is featured article if *Inverse Problems* in 2010.
- L. Beilina, M.V. Klibanov and M.Yu. Kokurin, Adaptivity with relaxation for ill-posed problems and global convergence for a coefficient inverse problem, *Journal of Mathematical Sciences, JMS*, Springer, 167, 279-325, 2010.
- L. Beilina, Adaptive Finite Element Method for a coefficient inverse problem for the Maxwell's system, *Applicable Analysis*, 90, 1461-1479, 2011.
- M.V. Klibanov, A.B. Bakushinskii and L. Beilina, Why a minimizer of the Tikhonov functional is closer to the exact solution than the first guess? *J. Inverse and Ill-posed problems*, 19, pp.83-105, 2011.
- L. Beilina and M.V. Klibanov, *Approximate Global Convergence and Adaptivity for Coefficient Inverse Problems*, Springer, New York, 2012.
- L. Beilina, Energy estimates and numerical verification of the stabilized domain decomposition finite element/finite difference approach for the Maxwell's system in time domain, *Central European Journal of Mathematics*, 11, 702-733, 2013.
- L. Beilina, Nguyen Trung Thành, M. V. Klibanov and M. A. Fiddy, Reconstruction from blind experimental data for an inverse problem for a hyperbolic equation, *Inverse Problems* 30, 025002, 2014.